G R A V I T Y D E F L E C T E D J E T S I N

T W O - D I M E N S I O N A L F L O W

A thesis presented at the

School of Engineering

University of Canterbury

In partial fulfilment

of the requirements for the degree

Master of Engineering

---

by

W. B. Fraser

May 1961

ACKNOWLEDGMENTS

Appreciation is here expressed to New Zealand Industrial Gases Limited for their generous financial assistance throughout the year.

Thanks are also extended to Mr F. M. Henderson for his continued guidance and encouragement during this work, and to Mr G. F. Archer for his assistance with the electrolytic plotting tank test.

TABLE OF CONTENTS

Table of Contents Contd.

LIST OF TABLES

LIST OF FIGURES

INTRODUCTION

Several attempts have been made to solve the hydrodynamical problem of calculating the exact shape of free surfaces deflected by gravity. As yet, no simple solution to the problem has been evolved. The most outstanding particular case of this problem, and one of considerable practical importance, is that of flow over a sharp-crested weir. This thesis investigates the possibility of applying a theorem developed by L.C. Woods to the weir problem, and in particular to its limiting cases of the free overfall and the weir of infinite depth.

After a brief account of previous research in Chapter I and a summary of Woods' theorem in Chapter II, the remainder of the thesis is devoted to the calculation of the free overfall profile. The profile obtained was found to differ somewhat from those obtained by other methods. Since all these methods are basically iterative processes, it is concluded that the convergence of such processes requires some investigation. As for Woods' theorem used in this way, the most that can be said at this stage is that it looks very promising.

NOMENCLATURE

(Symbols are listed approximately in their order of appearance in the text.)

z = $x + iy$ the physical plane

w = $\Phi + i\psi$ the complex potential plane

Φ the potential function

ψ the stream function

∇^2 = $\frac{\partial^2}{\partial x^2} + \frac{\partial^2}{\partial y^2}$ the Laplace operator

s distance along the stream lines

(q,θ) the velocity vector in polar coordinates

q_o the velocity of flow a great distance upstream from the weir

h the distance of the free surface below the total energy line (T.E.L.)

g acceleration due to gravity

f = $r + i\theta$

r = $\log \frac{q_o}{q}$

ζ = $\delta + i\xi$ Woods' auxiliary plane

y_o depth of the weir lip below the tangent to the free surface far upstream

d the depth of flow approaching the weir far upstream

A_{jk} terms of the integrand matrix

F Froude number

H = $y_o + \frac{q_o^2}{2g}$ height of total energy line above weir crest

$\frac{\partial \Phi}{\partial x} = \frac{\partial \psi}{\partial y}$ = x component of velocity = u

$\frac{\partial \Phi}{\partial y} = -\frac{\partial \psi}{\partial x}$ = y component of velocity = v

CHAPTER I

THE PROBLEM AND PREVIOUS RESEARCH

1.1 STATEMENT OF THE PROBLEM

If liquid flow can be assumed two dimensional and irrotational in a particular case, then there exists a complex potential function, $w = \Phi + i\psi$, such that,

$$\nabla^2\Phi = 0 = \nabla^2\psi \quad \text{---(1)}$$

Proof of this can be found in any standard text on hydrodynamics such as Milne-Thomson[2]. The problem now becomes that of solving Laplace's equation (equation 1) for particular boundary conditions. With reference to the weir problem, for example(Figure 1), these boundary conditions are:

(i) Boundaries AB, CDEF are streamlines (ψ = constant) and no flow can occur across these boundaries.

(ii) Along the free surface boundaries AB and CD the shape is unknown but the pressure is constant.

(iii) Applying Bernoulli's equation along AB, CD obtain,

$$\frac{d\Phi}{ds} = q = \sqrt{2gh} \quad \text{---(2)}$$

which must be satisfied at all points on the free surface.

Equation 2 implies that the velocity distribution along a free surface depends on its shape. Thus, solution of the problem requires knowledge of the answer.

1.2 INADEQUACY OF THE CLASSICAL TREATMENT

Kirchhoff's method of analysing flow with free surfaces springing

from solid boundaries can not be applied if the solid boundaries are curved, or if the free surfaces are deflected by gravity. He introduced the analytic function,

$$f = \log q_o \frac{dz}{dw}$$

$$= \log \frac{q_o}{q e^{-i\theta}}$$

$$= \log \frac{q_o}{q} + i\theta$$

$$= r + i\theta$$

This function maps straight solid boundaries on to lines parallel to the r axis of the f- plane, and free surfaces of constant velocity on to lines parallel to the θ axis. The resulting polygon in the f-plane can be mapped on to the complex potential plane using the Schwarz-Christoffel transformation. If the figure in the f-plane is not a polygon, as will be the case if the solid boundaries are curved and velocity varies on the free surface, this simple transformation cannot be used and the method fails.

1.3 DIRECT MATHEMATICAL TREATMENT

Mention should perhaps be made here of the work of Fritz John[3] and Hans Lewy[4] in developing exact mathematical solutions to the general problem of the gravity deflected free surface. A useful summary of these two papers is given by Milne-Thomson in reference 2, pp.301 ff.

In essence, both John and Lewy found that they could determine the solid boundary shapes which would produce a specified free surface. Both methods appear to be incapable of extension to anything other than single continuous free surfaces. They cannot, therefore, be used to

deal with jets and weirs. Results from these two methods have so far proved to be quite impractical from an engineering point of view, although mathematically they are most elegant. An example of flow with a parabolic free surface is given in Appendix A.

1.4 METHOD OF SOLUTION ADOPTED

From the considerations of section 1.1, the most obvious approach to the problem is to assume a free surface shape, calculate the boundary values equation 1 produces when applied to the flow region, and compare these values with those imposed by equation 2. On the basis of this comparison the assumed free surface shape can be adjusted and the process is repeated until agreement between the values is reached. This, of course, assumes that the process converges.

1.5 PREVIOUS RESEARCH

Previously, several results for free surface flows have been calculated using this general method. These can be classified according to the method used to calculate the boundary conditions produced by equation 1.

Relaxation methods: Southwell and Vaisey[5] have used relaxation methods to determine the profiles in several cases of free surface flows in two- and three-dimensions. Of particular interest here is their solution to the free overfall problem. In America, McNown, Hsu, and Yih[6] have applied the same methods to a case of particular interest, that of flow over a weir of infinite depth.

Electrolytic plotting tank methods: Hay and Markland[7] obtained profiles for the sharp crested weir by setting up the analogous situation in an

electrolytic plotting tank. Their results cover a range of weir depths including the extreme cases of free overfall and the weir of infinite depth.

Integration around the assumed boundary: If $f(\zeta)$ is a function of the complex variable ζ analytic inside and on a closed contour C, and z is a point inside C, then,

$$f(z) = \frac{1}{2\pi i} \int_C \frac{f(\zeta)}{\zeta - z} \, d\zeta$$

This is the Cauchy integral formula. The Cauchy integral formula can be used to obtain boundary values directly by numerical integration around the boundary. Lauck[8] has done this to obtain the profile of flow over a weir of infinite depth.

1.6 PRESENT METHOD OF SOLUTION

The method of solution presented in this thesis is similar to the method used by Lauck. In applying the Cauchy integral formula directly to the problem the integration must be carried out around a boundary that encloses the region exclusive of points at infinity. To accomplish this Lauck had to join the upper and lower bounding streamlines by carrying the integration across equipotential lines far upstream and far downstream respectively. An extension of the Cauchy integral formula by L.C. Woods[1] resolves this difficulty by confining the integration to the solid boundaries and the free surfaces.

Woods developed his theorem to analyse free surface flow with curved solid boundaries. In his paper he gives several examples, but in none of these are the effects of gravity considered. It is the purpose of this thesis to show how Woods' method of analysis can be applied when the free surface is deflected by gravity.

CHAPTER II

THE THEOREM OF L. C. WOODS

2.1 STATEMENT OF THE THEOREM

The infinite strip $0 \leqslant \psi \leqslant \psi_o$ in the w-plane represents flow in a channel of quite general type. The bounding streamlines $w = 0$, $w = \psi_o$ are boundaries on which either r or θ can be specified. (r is specified on the free surface, and θ on the solid boundary.) Consider now the infinite strip in the ζ-plane where boundaries on which r is specified map on to the line $\xi = \frac{\pi}{2}$, and those on which θ is specified map on to the line $\xi = 0$. The transformation between these two planes is achieved using the Schwarz-Christoffel theorem. Woods' theorem states that the analytic function $f(\zeta)$ is defined everywhere within, and on the boundary of the strip in the ζ-plane by the integral equation (equation 27 of reference 1),

$$f(\zeta) = r + i\theta$$

$$= r_\infty + i\theta_\infty + \frac{2}{\pi}\int_{\delta^*=-\infty}^{\infty} \tanh^{-1}\{\exp(\delta^* - \zeta)\}\, d\theta_o \quad (\delta^*)$$

$$- \frac{2}{\pi}\int_{\delta^*=-\infty}^{\infty} \tan^{-1}\{\exp(\delta^* - \zeta)\}\, dr_s \quad (\delta^*) \qquad ---(3)$$

The first integral is a line integral along $\xi = 0$, where θ is specified. If the solid boundary is straight θ = constant, and the first integral vanishes. The second integral is a line integral along

$\xi = \frac{\pi}{2}$ where r is specified. If the velocity is constant along the free surface, r = constant, and the second integral vanishes.

2.2 PROBLEMS INVOLVING GRAVITY

In problems where the free surfaces are deflected by gravity equation 3 can be used to calculate values of r and θ on the assumed boundary, that satisfy equation 1. These values of r and θ can be compared with those determined by equation 2. The assumed boundary can be adjusted and equation 3 applied again until agreement between boundary values from equation 3 and 2 is obtained. The convergence of the integrals and the iterative process is discussed in section 4.3.

Having outlined the general problem, and shown where Woods' theorem fits into the argument, the remainder of the thesis is concerned with particular examples.

CHAPTER III

THE SHARP-CRESTED WEIR

Figure 1 shows the general case of the sharp-crested weir and the two limiting cases. A solution has been obtained for the limiting case of the free overfall (Figure 9). In the case of the weir of infinite depth a solution could not be calculated because the integral in Woods' equation was divergent. A more general case for some specific value of $\frac{y_o}{d}$ other than one or zero was not attempted.

3.1 WOODS' THEOREM APPLIED

The mapping planes (z, w, and ζ) for the general case of the weir are shown in Figure 2. Since the solid boundaries are straight, the first integral vanishes except for a term due to the discontinuity in θ at E. Equation 3, for the weir, becomes,

$$f(\zeta) = r_D + i\theta_D + \tanh^{-1}\{\exp(\delta_E - \zeta)\} + \frac{2}{\pi}\int_{\delta^*=+\infty}^{-\infty} \tan^{-1}\{\exp(\delta^* - \zeta)\}\, dr_\varepsilon(\delta^*) \qquad ---(4)$$

In the limiting cases the term for the discontinuity at E is zero. For the free overfall $\theta_D = 0$, otherwise $\theta_D = \frac{\pi}{2}$ and in all cases $r_D = \log \frac{q_o}{q_D}$. The integration is carried out along the free surface in direction DCBA.

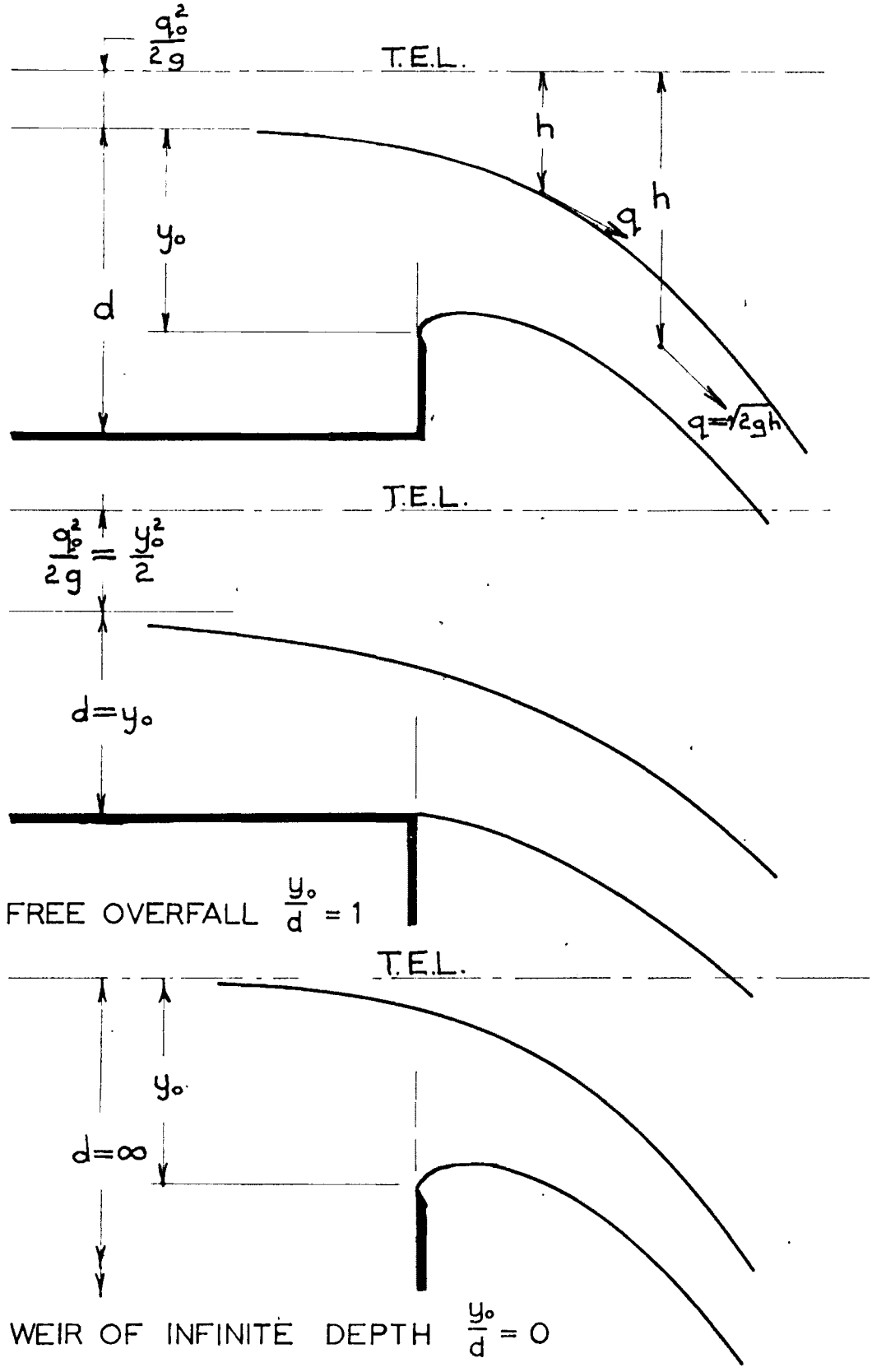

FIGURE 1

THE SHARP-CRESTED WEIR AND

ITS LIMITING CASES

The w - ζ transformation is given by the Schwarz-Christoffel theorem as,

$$\exp \zeta = \left\{ \exp\left(-\frac{\pi w}{\psi_o}\right) - 1 \right\}^{-\frac{1}{2}} \qquad ---(5)$$

On the free surface $\zeta^* = \delta^* + i\frac{\pi}{2}$ and,

$$\exp \delta^* = -i \left\{ \exp\left(-\frac{\pi w^*}{\psi_o}\right) - 1 \right\}^{-\frac{1}{2}}$$

Thus the integrand of equation 4 becomes,

$$\tan^{-1}\{\exp(\delta^* - \zeta)\} = -i \tanh^{-1} \left\{ \frac{\exp\left(-\frac{\pi w}{\psi_o}\right) - 1}{\exp\left(-\frac{\pi w^*}{\psi_o}\right) - 1} \right\}^{\frac{1}{2}} \qquad ---(6)$$

Since the functional relationship between the integrand and r is not known, the integral must be evaluated by a numerical process. Equal steps in potential, $\Delta\Phi$, are set along the boundaries and the value of the integrand at the mid-point of each interval is calculated. This leads to the matrix A_{jk} (Table II), where k varies with w and is the point for which $f(\zeta)$ is being evaluated. j varies with w*.

$$A_{jk} = \tanh^{-1} \frac{\beta_k}{\beta_j}$$

$$\beta_k = \left\{ \exp\left(-\frac{\pi w}{\psi_o}\right) - 1 \right\}^{\frac{1}{2}} \qquad ---$$

$$\beta_j = \left\{ \exp\left(-\frac{\pi w^*}{\psi_o}\right) - 1 \right\}^{\frac{1}{2}} \qquad ---(7)$$

In terms of finite differences, equation 4 becomes,

$$f(\zeta_k) = r_D + i\theta_D + \tanh^{-1}\{\exp(\delta_E - \zeta_k)\} - \frac{2i}{\pi} \sum_{j=1}^{N} A_{jk}(\Delta r)_j \qquad ---(8)$$

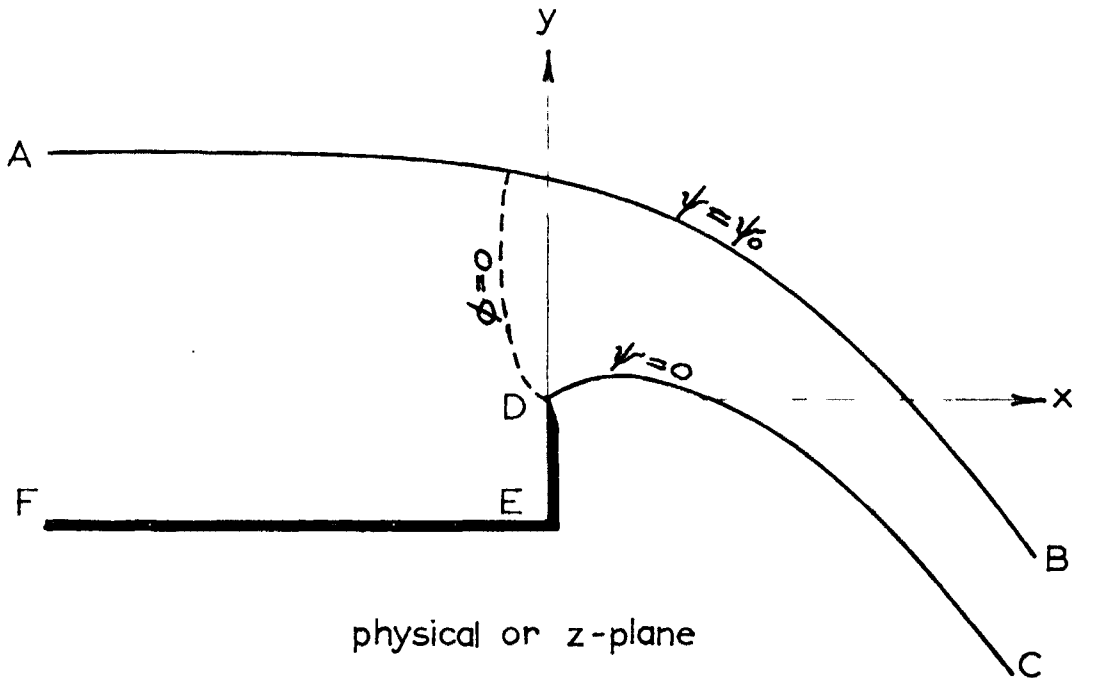

physical or z-plane

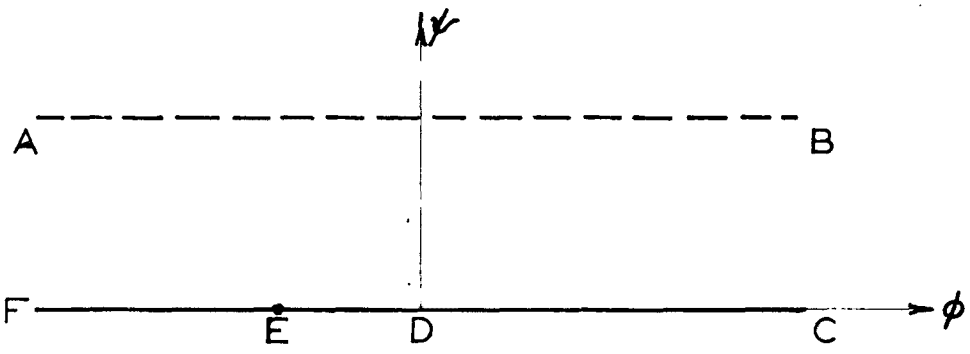

complex potential or w-plane

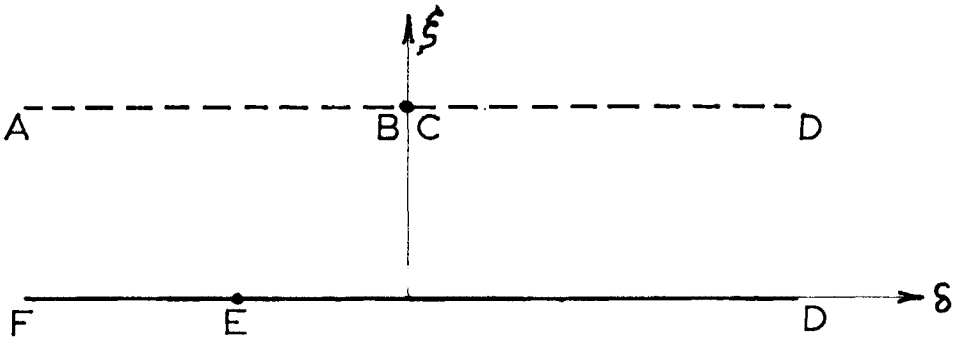

auxiliary or ζ-plane

FIGURE 2

MAPPING PLANES FOR

THE SHARP-CRESTED WEIR

The integrand A_{jk} is independent of the assumed shape and is the same for all cases of the weir problem. Thus, once calculated the matrix can be used for successive trials in a particular case, and for all cases. The matrix in Table II was calculated by F. M. Henderson, senior lecturer in civil engineering at the University of Canterbury.

$(\Delta r)_j$ is not a constant increment during the summation, but varies with the position j and the assumed shape. Values of $(\Delta r)_j$ corresponding to the $\Delta\Phi$ intervals can be calculated from equation 2 for particular trial shapes. The summations can then be carried out and the new values produced can be compared with the ones from equation 2.

3.2 CALCULATION OF THE INTEGRAND MATRIX

The interval of integration was chosen to be $\Delta\Phi = \frac{\psi_o}{4}$, ψ_o being the stream function value on the upper boundary. Values of the integrand calculated for these intervals are then independent of the absolute magnitude of w. Table 1 sets out values of β calculated from equation 7. Inspection of Table 1 shows that β is always positive, imaginary, and increases as j increases. The calculation of $\tanh^{-1}\frac{\beta_k}{\beta_j}$ will depend, therefore, on whether $j > k$, $j < k$, or $j = k$.

$j > k$: If $j > k$, then $\frac{\beta_k}{\beta_j} < 1$, and $\tanh^{-1}\frac{\beta_k}{\beta_j}$ is pure real.

$j < k$: If $j < k$, then $\frac{\beta_k}{\beta_j} > 1$, and

$$\tanh^{-1}\frac{\beta_k}{\beta_j} = \tanh^{-1}\frac{\beta_j}{\beta_k} + i\frac{\pi}{2}$$

where the first term on the right-hand side is pure real and the imaginary term is constant for all $1 < j < k$. Hence the imaginary

term will make a contribution to the summation of,

$$\frac{2i}{\pi} \sum_{j=1}^{k} i \frac{\pi}{2} (\Delta r)_j = - \sum_{j=1}^{k} (\Delta r)_j$$

$$= \text{total change in r between D and k}$$

$$= r_D - r_k$$

$\underline{j = k}$: If $j = k$, then $\frac{\beta_k}{\beta_j} = 1$, and $\tanh^{-1} \frac{\beta_k}{\beta_j}$ is infinite. However, although the integrand at this point is infinite, the summation is still finite. A value obtained by pure integration has, therefore, to be inserted into the summation here. To do this the argument $(\frac{\beta_k}{\beta_j})$ needs to be known as a function of r. Since the contribution of this term to the summation is small it will be assumed that this relationship is linear, and an "average ordinate", A_{kk}, is calculated and inserted into the matrix at all points $j = k$. For the details of this see Appendix B.

The summation is thus broken into its several components and equation 8 can be written in detailed form,

$$f(\zeta_k) = r_k + i\theta_k$$

$$= r_D + i\theta_D + \tanh^{-1} \{\exp (\delta_E - \zeta_k)\}$$
$$- i \frac{2}{\pi} \sum_{j=1}^{k-1} \tanh^{-1} \frac{\beta_j}{\beta_k} (\Delta r)_j - r_D + r_k$$
$$- i \frac{2}{\pi} \sum_{j=k+1}^{N} \tanh^{-1} \frac{\beta_k}{\beta_j} (\Delta r)_j - i \frac{2}{\pi} A_{kk} (\Delta r)_k$$

Which simplifies, putting,

$$A_{jk} = \tanh \frac{\beta_k}{\beta_j} \text{ , or } A_{kk} \text{ if } j = k$$

to

$$\theta_k = \theta_D - \frac{2}{\pi} \sum_{j=1}^{N} A_{jk} (\Delta r)_j \qquad ---(9)$$

Equation 9 produces new values of θ only, to be compared with the values of θ and r specified by equation 2. Applying equation 2 and

$$\frac{dh}{ds} = \sin \theta \qquad ---(10)$$

to these new values of θ, corresponding values of r, and hence Δr, can be calculated to produce a new trial surface.

3.3 RANGE OF SUMMATION

Something must now be said about the upper limit of the summation, j = N. Theoretically an infinite number of steps should be taken as the summation proceeds downstream along DC and upstream again along BA. It is convenient to start the summation at the weir crest D since at this point Φ, r, and θ are known.

Downstream limit: Far downstream $\beta_j \to 1$ and,

$$A_{jk} = \left| \tanh^{-1} \frac{\beta_k}{\beta_j} \right| \to \left| \tanh^{-1} \beta_k \right| = \text{constant} \qquad ---(11)$$

provided $\beta_k \not\to \beta_j$, i.e. $\frac{\beta_k}{\beta_j} \not\to 1$. There will be an equipotential far downstream at n after which the integrand, for the purposes of the summation, can be assumed constant. Its contribution to the summation after this equipotential will be,

$$\Sigma \tanh^{-1} \beta_k \ (\Delta r) = \tanh^{-1} \beta_k \ \Sigma \ \Delta r$$

$$= A_{nk} \times \text{difference in r across the equipotential at n}$$

Hence the summation is carried downstream until the integrand is constant and then a jump from the lower to the upper boundary is made.

TABLE I - VALUES OF β WHEN $\Delta\Phi = \frac{\psi_o}{4}$

	j,k	mid-interval values of w/ψ_o	$\exp\left(-\frac{\pi w}{\psi_o}\right)$	$\beta = \left\{\exp\left(-\frac{\pi w}{\psi_o}\right) - 1\right\}^{\frac{1}{2}}$
Lower free stream line	1	$\frac{1}{8}$	+ 0.6758	i 0.5698
	2	$\frac{3}{8}$	+ 0.3078	i 0.8320
	3	$\frac{5}{8}$	+ 0.1403	i 0.9272
	4	$\frac{7}{8}$	+ 0.06404	i 0.9674
	5	$1\frac{1}{8}$	+ 0.02920	i 0.9853
	6	$1\frac{3}{8}$	+ 0.01330	i 0.99333
	7	$1\frac{5}{8}$	+ 0.006065	i 0.996968
	8	$1\frac{7}{8}$	+ 0.002766	i 0.998617
	9	$2\frac{1}{8}$	+ 0.001261	i 0.9993697
	10	$2\frac{3}{8}$	+ 0.0005751	i 0.9997124
	11	$2\frac{5}{8}$	+ 0.0002623	i 0.9998688
	12	$2\frac{7}{8}$	+ 0.0001196	i 0.9999402
Upper free stream line	13	i + $2\frac{7}{8}$	- 0.0001196	i 1.00005980
	14	i + $2\frac{5}{8}$	- 0.0002623	i 1.0001311
	15	i + $2\frac{3}{8}$	- 0.0005751	i 1.0002875
	16	i + $2\frac{1}{8}$	- 0.001261	i 1.0006302
	17	i + $1\frac{7}{8}$	- 0.002766	i 1.001382
	18	i + $1\frac{5}{8}$	- 0.006065	i 1.003027
	19	i + $1\frac{3}{8}$	- 0.01330	i 1.00665
	20	i + $1\frac{1}{8}$	- 0.02920	i 1.0144
	21	i + $\frac{7}{8}$	- 0.06404	i 1.0315
	22	i + $\frac{5}{8}$	- 0.1403	i 1.0677
	23	i + $\frac{3}{8}$	- 0.3078	i 1.1435
	24	i + $\frac{1}{8}$	- 0.6753	i 1.2945
	25	i - $\frac{1}{8}$	- 1.481	i 1.575
	26	i - $\frac{3}{8}$	- 3.248	i 2.061
	27	i - $\frac{5}{8}$	- 7.124	i 2.850
	28	i - $\frac{7}{8}$	- 15.64	i 4.080
	29	i - $1\frac{1}{8}$	- 34.25	i 5.9375
	30	i - $1\frac{3}{8}$	- 75.19	i 8.7285
	31	i - $1\frac{5}{8}$	- 164.85	i 12.88
	32	i - $1\frac{7}{8}$	- 361.5	i 19.04

TABLE II - MATRIX OF INTEGRAND $A_{jk} \times 10^4$

Lower Free Stream Line	j \ k	Lower Free Stream Line								Upper Free Stream Line											
		1	2	3	4	5	6	7	8	17	18	19	20	21	22	23	24	25	26	27	28
	1	8520	8390	7140	6760	6600	6540	6510	6490	6470	6450	6504	6353	6220	5949	5570	4725	3792	2831	2028	1366
	2	8360	19550	14550	12930	12340	12120	12030	11980	11940	11900	11760	11600	11170	10400	9230	7630	5875	4287	3006	2062
	3	7140	14540	24800	19260	17480	16850	16600	16500	16300	16200	15960	15520	14640	13210	11300	9000	6740	4849	3378	2306
	4	6760	12900	19260	29900	23450	21630	20960	20700	20300	20070	19600	18700	17200	15040	12400	9660	7150	5091	3536	2410
	5	6598	12330	17490	23460	33460	27500	25650	25050	24060	23600	22660	21140	18890	16070	13000	9950	7310	5203	3607	2455
	6	6526	12110	16850	21620	27560	37510	31520	29680	27570	26490	25030	22760	19860	16630	13220	10100	7400	5260	3640	2476
	7	6449	12020	16610	20960	25900	31500	41600	35440	30600	29010	26650	23750	20380	16870	13450	10180	7440	5282	3653	2485
	8	6486	11990	16500	20700	25040	29680	35490	45460	32950	30580	27600	24220	20630	16990	13500	10200	7460	5294	3660	2489
	9	6480	11970	16460	20600	24720	29010	33600	44740	34500	31260	28100	24500	20720	17030	13530	10220	7480	5299	3663	2491
	10	6476	11960	16430	20530	24600	28740	32930	37940	35370	32010	28400	24600	20780	17060	13560	10240	7490	5302	3664	2492
	11	6475	11960	16410	20510	24550	28630	32650	37890	35900	32240	28540	24600	20810	17080	13580	10250	7500	5302	3665	2493
	12	6474	11950	16410	20510	24550	28580	32520	36590	36100	32360	28610	24720	20850	17100	13580	10250	7502	5303	3665	2493
	13	6474	11950	16400	20460	24500	28520	32340	36100	36590	32550	28610	24720	20850	17100	13580	10250	7502	5303	3665	2493
	14	6473	11950	16400	20460	24500	28430	32220	35900	37890	32670	28660	24720	20850	17100	13580	10250	7502	5304	3665	2493
	15	6471	11950	16380	20440	24430	28300	31990	35370	37940	32960	28770	24800	20870	17110	13580	10250	7507	5304	3666	2494
	16	6468	11940	16360	20410	24330	28060	31240	39500	44930	33620	29010	24880	20930	17140	13590	10260	7513	5306	3667	2494
	17	6462	11920	16300	20300	24070	27570	30580	32950	45490	35510	29700	25230	21050	17180	13600	10270	7520	5310	3670	2496
	18	6450	11890	16200	20080	23600	26640	29010	30600	35530	41570	31600	25900	21330	17330	13650	10290	7532	5319	3678	2500
	19	6410	11800	15960	19600	22670	28240	26670	27610	29700	31600	38770	27880	22030	17630	13840	10350	7570	5340	3693	2506
	20	6330	11600	15520	18700	21120	22470	23740	24220	25200	25900	27880	33930	23650	18290	14100	10500	7640	4969	3725	2540
	21	6220	11150	14640	17200	18890	19860	20370	20620	21040	21330	22030	23650	30000	20270	14830	10880	7848	5502	3800	2590
	22	5950	10380	13250	15050	16090	16610	16880	17000	17200	17340	17640	18320	20270	27000	16880	11740	8240	5735	3940	2690
	23	5469	9250	11300	12400	13000	13220	13420	13460	13600	13650	13830	14100	14830	16880	23700	13930	9200	6244	4270	2870
	24	4722	7610	9000	9660	9960	10120	10180	10210	10270	10290	10360	10500	10890	9180	13930	21480	11650	7380	4860	3245
	25	3791	5877	6757	7130	7330	7410	7460	7470	7500	7520	7380	7620	7820	8250	9200	11660	19640	10020	6220	4060
	26	2847	4283	4846	5089	5201	5252	5278	5285	5309	5317	5334	5386	5501	5726	6260	7350	10030	18500	9140	5540
	27	2025	3005	3376	3534	3607	3638	3656	3662	3673	3678	3692	3724	3793	3924	4254	4900	6210	9140	17640	8640
	28	1407	2068	2314	2418	2466	2487	2497	2801	2507	2511	2520	2540	2586	2680	2880	3287	4074	5573	8650	17300
	29	962	1411	1576	1644	1675	1689	1695	1698	1703	1705	1711	1725	1755	1818	1950	2216	2718	3621	5200	8420
	30	654	956	1066	1112	1133	1143	1147	1149	1152	1154	1158	1168	1187	1229	1318	1494	1825	2407	3380	5040
	31	444	647	721	752	767	773	776	777	779	780	783	789	802	830	888	1008	1229	1615	2250	3280
Upper Free Stream Line	32	300	437	488	509	518	522	524	525	526	527	529	533	542	560	601	681	829	1087	1500	2175

If $\frac{\beta_k}{\beta_j} \to 1$, equation 11 is not valid, as $\tanh^{-1} x$ is very sensitive to changes in x as $x \to 1$. β_j must therefore be carried farther downstream than β_k. Put $\frac{\beta_k}{\beta_n} = x$

$$\frac{d}{dx}(\tanh^{-1} x) = \frac{1}{1 - x^2}$$

$$\frac{d(\tanh^{-1} x)}{\tanh^{-1} x} \Big/ \frac{dx}{x} = \frac{x}{(1 - x^2)\tanh^{-1} x}$$

Put $x = 1 - \varepsilon$ and let $\varepsilon \to 0$ $(\beta_k \to \beta_n)$

$$\frac{d(\tanh^{-1} x)}{\tanh^{-1} x} \Big/ \frac{dx}{x} = \frac{1}{\varepsilon \log \frac{2}{\varepsilon}} \qquad \text{---(12)}$$

If the extreme value of k is $k = 8$ and if $n = 12$, then the variation in the constancy of the integrand at this point is 0.032 (by equation 12) which amounts to less than 1% of the summation.

Upstream limit: As the summation proceeds upstream towards A, the integrand is decreasing provided $j > k$, and this can always be arranged. More important is the fact that

$$\Delta r = \Delta \log \frac{q_o}{q} = \frac{\Delta q}{q} = \frac{\Delta h}{2h} \to 0$$

because $\Delta h \to 0$, upstream, except in the case of the weir of infinite depth when both Δh and h tend to zero.

3.4 THE WEIR OF INFINITE DEPTH

If Δh tends to zero more rapidly than h tends to zero at the upstream end of the weir of infinite depth, then the summation converges. However values of Δr based on the profile obtained by McNown, Hsu, and Yih[6] were found to diverge in this region. Further, the integrand does not converge rapidly enough to make the summation convergent. Values of the terms of

TABLE III

TERMS OF SUMMATION AT UPSTREAM END OF WEIR OF INFINITE DEPTH

$\frac{\Phi}{\Psi_o}$	$(\Delta r)_j$	k = 1		k = 24		k = 26	
		A_{jk}	$A_{jk}(\Delta r)_j$	A_{jk}	$A_{jk}(\Delta r)_j$	A_{jk}	$A_{jk}(\Delta r)_j$
1/16	0.0825	0.4032	0.0333	1.3306	0.1098	0.9129	0.0753
1/8	0.0725	0.3790	0.0275	1.1626	0.0843	1.0062	0.0729
3/16	0.0675	0.3545	0.0239	1.0285	0.0694	1.1335	0.0765
1/4	0.0660	0.3304	0.0218	0.9168	0.0605	1.3213	0.0872
5/16	0.0675	0.3067	0.0207	0.8213	0.0554	1.6540	0.1116
3/8	0.0730	0.2838	0.0207	0.7383	0.0539	1.8500	0.1351
7/16	0.0815	0.2618	0.0213	0.6649	0.0542	1.6296	0.1328
1/2	0.0930	0.2405	0.0224	0.5999	0.0558	1.2744	0.1185
9/16	0.1090	0.2215	0.0241	0.5413	0.0590	1.0640	0.1160
5/8	0.1280	0.2027	0.0259	0.4897	0.0627	0.9139	0.1170
11/16	0.1540	0.1851	0.0285	0.4428	0.0682	0.7981	0.1229
3/4	0.1850	0.1696	0.0314	0.4012	0.0742	0.7035	0.1301

the summation are given in Table III for a representative range of values of k. It must be concluded that this case of weir flow cannot be analysed by Woods' method.

3.5 WEIRS OF FINITE DEPTH

In all other cases Δr will tend to zero upstream and the summation will converge. However, except in the free overfall case, not only is the free surface shape unknown, but the discharge and the value of Φ at the discontinuity E are indeterminate. Three initial assumptions must be made, and in the iteration all three of these may have to be varied. Since Woods' equation produces new values of θ only, the way in which discharge and potential at E should be adjusted will be largely a matter of guess-work.

Although these three factors are not independent their relationship depends on knowing the z - w relationship, which is basically what is being established by the process. A specific example of this nature was not attempted.

CHAPTER IV

THE FREE OVERFALL

For the free overfall the method was carried to its conclusion and a result was obtained. Figure 9 shows this resultant profile plotted with profiles obtained by other workers for comparison.

In the case of the free overfall the number of unknowns is reduced and the iterative process is thereby simplified. Far upstream the flow is at "critical depth" and the discharge and velocity are known exactly. The discontinuity term due to the change in direction of the solid boundary at E no longer exists, and the only unknown property of the flow is the free surface shape.

4.1 THE UNIT MODEL

Use of the unit model in which $g = 1$ and $y_o = 1$ reduces the numerical calculations for $(\Delta r)_j$ significantly. Flow over weirs of the same ratio $\frac{y_o}{d}$ will have geometrically similar profiles, and have the same characteristic Froude number,

$$F^2 = \frac{q^2}{gy}$$

Provided a suitable scale factor is introduced for the velocity term, g can be chosen to have any arbitrary value without effecting this geometrical similarity. Hence, results obtained for the unit model can be applied to the corresponding real flow situation by the following transformations. (Superscripted letters refer to the unit model.)

$$x = x' y_o$$

$$y = y' y_o$$

$$q = q' \sqrt{g y_o}$$

$$\Phi = \Phi' \, y_o \sqrt{g y_o}$$

$$\psi = \psi' \, y_o \sqrt{g y_o}$$

and equation 2 becomes

$$\frac{d\Phi'}{ds'} = q' = \sqrt{2h'} \qquad \text{---(13)}$$

In the remainder of this chapter the superscripts will be dropped and all values will refer to the unit model.

4.2 CALCULATION OF $(\Delta r)_j$ FOR SUCCESSIVE TRIAL SHAPES

As a starting point for the iteration the profile obtained by Hay and Markland[7] in the electrolytic tank was used. First trial values of $(\Delta r)_j$ were calculated using equation 13 by setting off Δs along the curve and measuring the corresponding value of h. Since j extends further downstream than k, the new values of θ obtained cover a smaller range than required for calculating corresponding values of $(\Delta r)_j$ to use in the second trial. For the first four trials the new profiles were plotted and it was then a simple matter to extrapolate from j = 8 to j = 12. A simpler method, and one that is certainly as accurate, is to plot $(\Delta r)_j$ against j (Figure 3). A "smoothing" curve drawn through these values can be extrapolated to cover the whole range of integration. This method was adopted for the last three iterations.

Having arrived at position j = 12 on the lower free surface, it is

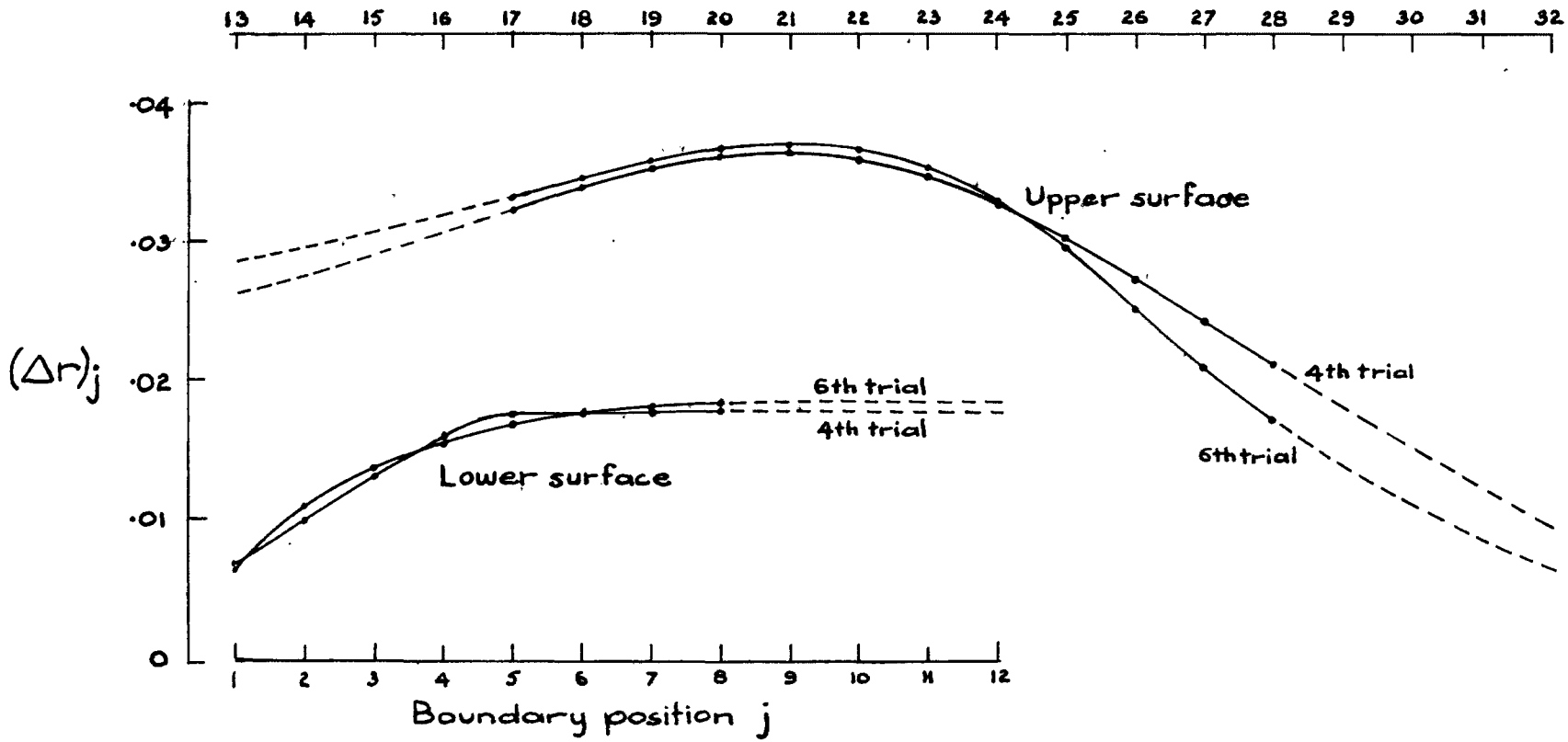

FIGURE 3
SMOOTHING CURVE FOR Δr INCREMENTS

necessary to establish position j = 13 on the upper free surface. This was done using the equations,

$$\Delta h = \frac{2}{3} y_o \cos^2 \bar{\theta}$$
$$\Delta x = \Delta h \sin \bar{\theta} \qquad \text{---(14)}$$

$\bar{\theta}$ is the average value of θ across the equipotential. Once position j = 13 is established the calculation back along the upper free surface proceeds as it did for the lower free surface.

The first equation 14 is derived from energy and momentum considerations on the assumption that the pressure in the jet is constant and equal to the external pressure on the free surfaces. At a sufficient distance downstream from the overfall edge this is true. The distance is such that $\frac{x}{H} > 0.5$ according to Ven Te Chow[9]. The derivation of this equation is set out in Appendix C.

4.3 CONVERGENCE

Two of the conditions that must be satisfied before Woods' theorem can be successfully applied to a flow problem relate to convergence. Firstly the summation $\Sigma A_{jk}(\Delta r)_j$ must converge to a finite sum. In the case of the weir of infinite depth this condition was not satisfied. Secondly the iterative process itself must converge. That is, successive trial shapes must be more and more nearly coincident, converging to a unique final shape which will be the solution. It is possible that successive trial shapes will oscillate infinitely.

The problem of how to determine whether or not a particular iterative process will converge, without actually carrying it out, is in this case

unable to be solved, as the behaviour of the various parameters involved depends directly on the assumed surface shape. Indeed, it may be that if the assumed shape is grossly in error the process will not converge even though it may converge if the initial assumption is close to the true solution. This problem is common to all of the three methods mentioned in section 1.5. However, no previous workers have discussed this matter extensively. Generally the conclusion is that if a process is found to converge when it is applied to a particular problem then the application is justified.

In the case of the free overfall, solved by Woods' method, the convergence of the iteration was found to be very slow. It was made more rapid by averaging the θ values obtained in the second and third trials for use in the fourth trial. Inspection of Figure 9 will give some indication of how close the convergence had become when the iteration was halted. Table IV sets out the co-ordinates calculated for the final two trials.

The result thus obtained is substantially different from that of Hay and Markland[7]. (Also plotted in Figure 9; this profile is almost identical with the one obtained by Southwell and Vaisey[5] by relaxation.) This could, of course, be due to inaccuracy of the integrand matrix or the limit of the range of integration, which would presumably lead to a result slightly different from the true one. However, a completely independent approximate check can be devised very simply. The medians of the meshes of a flow net are equal, and since the curvature of the stream lines and equipotentials in the flow field of the free overfall is slight, to a fairly close degree of approximation, it can be stated

that:

the average jet width between adjacent equipotentials (spaced at $\Delta\Phi = \frac{\Psi_o}{4}$) is equal to four times the average distance along the free surfaces between the equipotentials.

Equation 13 can be used to obtain the $\Delta\Phi$ steps on the free surfaces, and this was done for both Hay and Markland's profile and the profile obtained in this thesis (see reduced diagrams in Figures 4 and 5). The points thus obtained are compatible with the boundary condition of equation 2. Application of the above test then gives an approximate check as to how well equation 1 is satisfied. The results of this test are tabulated in Table V. For both profiles the difference between jet width and four times the surface increment is small, the agreement in the present case being better than for Hay and Markland's profile.

4.4 ELECTROLYTIC PLOTTING TANK TEST

As a final check the profile obtained was set up in a plotting tank and the potential distribution around the boundary was measured. The results are set out in Table VI. The maximum difference between the calculated and plotting tank results is 0.007, which represents 0.2% of the total voltage across the tank. Since the voltage cannot be measured more accurately than this (although sensitivity of the potentiometer is such that voltage variations of 0.1% could be detected) it may be stated that the profile calculated by Woods' method is true within the limits of accuracy set by this test. The accuracy attained in this plotting tank is comparable with the work of Hay and Markland.

TABLE IV

CO-ORDINATES OF FREE OVERFALL PENULTIMATE AND ACCEPTED PROFILES

	6th trial		7th trial	
	x	h	x	h
Lower Stream line	0	1.500	0	1.500
	0.143	1.520	0.143	1.519
	0.281	1.533	0.282	1.552
	0.415	1.596	0.416	1.594
	0.545	1.646	0.546	1.643
	0.669	1.703	0.671	1.699
	0.788	1.765	0.791	1.760
	0.902	1.831	0.906	1.825
	1.012	1.899	1.017	1.892
Upper Stream line	1.327	1.452	1.328	1.440
	1.211	1.359	1.210	1.348
	1.085	1.270	1.083	1.259
	0.952	1.182	0.948	1.173
	0.809	1.099	0.804	1.090
	0.656	1.020	0.650	1.013
	0.493	0.948	0.485	0.942
	0.320	0.883	0.312	0.877
	0.137	0.826	0.128	0.822
	-0.055	0.779	-0.064	0.775
	-0.254	0.740	-0.269	0.737
	-0.459	0.709	-0.475	0.707
	-0.669	0.684	-0.685	0.683

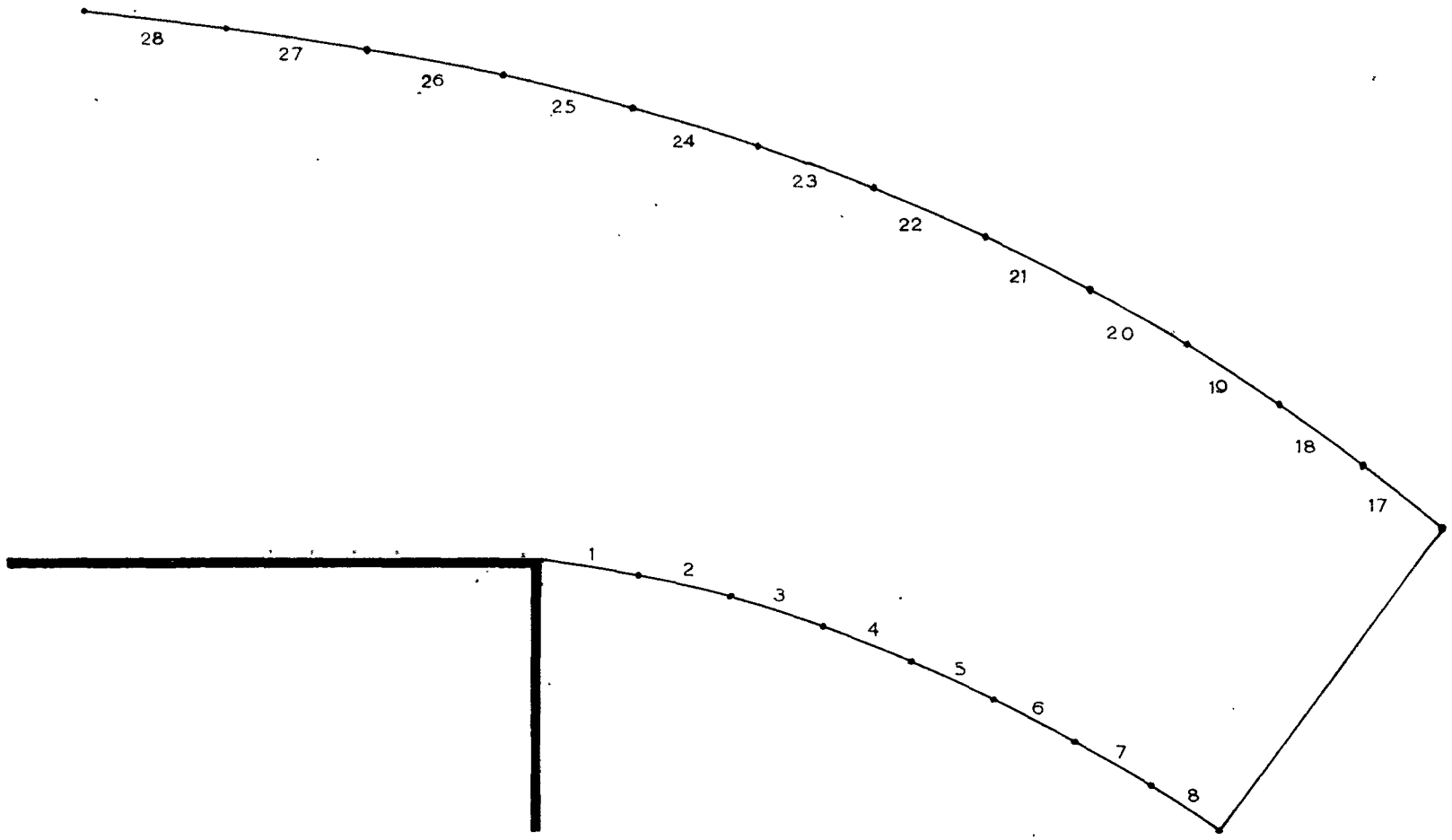

FIGURE 4

FREE OVERFALL PROFILE USING WOODS' THEOREM

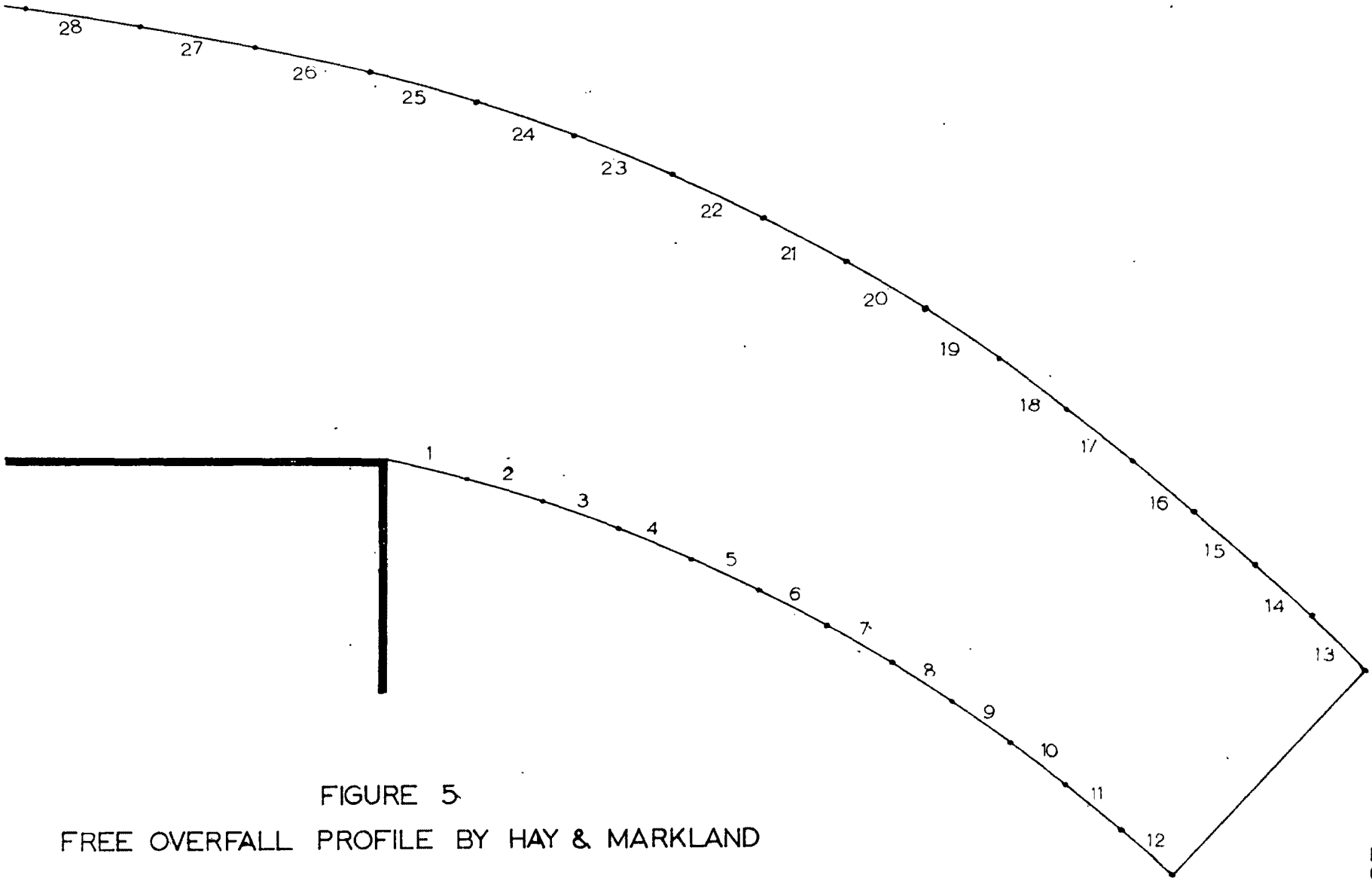

FIGURE 5

FREE OVERFALL PROFILE BY HAY & MARKLAND

TABLE V

APPROXIMATE TEST FOR ACCURACY OF PROFILES

profile section	Hay and Markland					
	average jet width	4 x average value of Δs	difference %	average jet width	4 x average value of Δs	difference %
13 - 12	0.498	0.498	0			
14 - 11	0.506	0.510	0.8			
15 - 10	0.516	0.522	1.2			
16 - 9	0.528	0.536	1.5			
17 - 8	0.540	0.546	1.1	0.559	0.560	0.2
18 - 7	0.551	0.564	2.4	0.569	0.574	0.9
19 - 6	0.565	0.576	2.0	0.588	0.588	0
20 - 5	0.580	0.588	1.4	0.604	0.602	-0.3
21 - 4	0.594	0.610	2.7	0.619	0.622	0.5
22 - 3	0.611	0.624	2.1	0.635	0.636	0.2
23 - 2	0.629	0.642	2.1	0.654	0.652	-0.3
24 - 1	0.643	0.656	2.0	0.677	0.674	-0.4

TABLE VI

ELECTROLYTIC PLOTTING TANK RESULTS

	j	$\Delta\Phi$ used in calculations	$\Delta\Phi$ measured in plotting tank	difference
Lower surface	1	0.25	0.247	-0.003
	2	0.25	0.243	-0.007
	3	0.25	0.250	0.000
	4	0.25	0.247	-0.003
	5	0.25	0.248	-0.002
	6	0.25	0.250	0.000
	7	0.25	0.252	+0.002
Upper surface	18	0.25	0.248	-0.002
	19	0.25	0.248	-0.002
	20	0.25	0.247	-0.003
	21	0.25	0.250	0.000
	22	0.25	0.245	-0.005
	23	0.25	0.248	-0.002
	24	0.25	0.247	-0.003
	25	0.25	0.248	-0.002
	26	0.25	0.255	+0.005
	27	0.25	0.252	+0.002
	28	0.25	0.250	0.000

CHAPTER V

CONCLUSIONS

As explained in Chapter I the problem of gravity deflected jets dealt with here is one of solving Laplace's equation for certain boundary conditions. The use of Woods' theorem, as against relaxation techniques or electrolytic plotting tank methods, is the most direct method since it yields directly, information about boundary values. Relaxation, on the other hand, has to be applied to the whole field of flow before boundary values can be derived.

The profile of the free overfall calculated in this thesis is found to differ significantly from the profile obtained by Hay and Markland in the electrolytic plotting tank and that of Southwell and Vaisey calculated by relaxation. The independent tests applied to the profile, as calculated using Woods' method, indicate that it is at least as good as these others. It is interesting to note that the upper free surface shape obtained agrees very well with the experimental profile obtained by Rouse[10], and that the experimental profile of the lower free surface lies approximately midway between the profile of Hay and Markland and the one calculated here (see Figure 9). This suggests that the question of the convergence of these iterative processes should be examined more fully.

Unfortunately there has been time only to carry the solution of one problem through to a successful conclusion. Before full confidence can

be expressed in this method it will be necessary to apply it to other problems for which results are available from other sources. One such problem, which is of some practical interest, is the gravity deflected jet issuing from a horizontal slot in a vertical plate.

Woods' theorem applied in this way looks very promising. Although the work involved is lengthy it is certainly no more so than that involved in relaxation or electrolytic plotting tank methods. The possibility of using a digital computer for this problem is worth considering as computers are particularly suitable for such repetitive calculation. Provided some numerical method of extending the range of derived boundary values to cover the same range as the initially assumed values can be found the use of a computer should be feasible.

REFERENCES

1 WOODS, L.C. "Compressible Subsonic Flow in Two-Dimensional Channels with Mixed Boundary Conditions" Quart. J. Mech. and App. Math., Vol. VII, Pt. 3, (1945) p. 263.

2 MILNE-THOMSON, L.M. "Theoretical Hydrodynamics" 4th ed., Macmillan, Lond. (1960).

3 JOHN, Fritz "Two-Dimensional Potential Flows with a Free Boundary" Comm. Pure and Applied Math., Vol. VI (1953) p. 413.

4 LEWY, Hans "On Steady Free Surface Flow in a Gravity Field" Comm. Pure and Applied Math., Vol. V (1952) p. 413.

5 SOUTHWELL, R.V. and VAISEY, G. "Relaxation Methods Applied to Engineering Problems XII Fluid Motions Characterized by Free Stream-Lines" Phil. Trans. Roy. Soc., Series A, Vol. 240 (1946) p. 117.

6 McNOWN, J.S., En-Yun HSU, and Chia-Shun YIH "Applications of the Relaxation Technique in Fluid Mechanics" Trans. Amer. Soc. Civ. Engrs, Vol. 120 (1955) p. 650.

7 HAY, N. and E. MARKLAND "The Determination of the Discharge Over Weirs by the Electrolytic Tank" Proc. Inst. Civ. Engrs, Vol. X (1957) p. 59.

8 LAUCK, A. "Der Uberfall über ein Wehr" Z. angew. Math. Mech., Vol. 5 (1925) p. 1.

9 VEN TE CHOW "Open-channel Hydraulics" McGraw-Hill, New York (1959).

10 MORE, W.L. "Energy Loss at the Base of a Free Overfall" Trans. Amer. Soc. Civ. Engrs, Vol. 108 (1943) p. 1343.

Reference is made here to a discussion, by Rouse, of this paper.

APPENDICES

APPENDIX A

FLOW WITH A PARABOLIC FREE SURFACE BY THE METHOD OF FRITZ JOHN[3]

The free surface of a two-dimensional steady flow is a curve C given by the equation $z = F(\alpha)$ where α is a real valued Lagrangian co-ordinate. On C the Euler equation of fluid flow can be written as,

$$\frac{d^2F}{d\alpha^2} + ig = i\,G(\alpha)\frac{dF}{d\alpha} \qquad \text{---(I)}$$

(equation 5 of John's paper)

Further, if the flow is irrotational with complex potential w, then on C

$$\frac{dw}{d\alpha} = \frac{d\bar{F}}{d\bar{\alpha}} \cdot \frac{dF}{d\alpha} \qquad \text{---(II)}$$

(equation 6 of John's paper)

If now it is assumed that $z = F(\alpha)$ is an analytic function of α then equation II can be used to define w for complex values of α. The complex potential $w(\alpha)$ so defined will be the complex potential of a flow which is consistent with the free surface given by $z = F(\alpha)$.

The simplest possible solution to equation I is obtained if

$$G(\alpha) = 0$$

$$\frac{d^2F}{d\alpha^2} = -ig$$

$$\frac{dF}{d\alpha} = -ig\alpha + A$$

$$F = -i\tfrac{1}{2}g\alpha^2 + A\alpha + B$$

This is a parabolic surface and if the origin is taken at the apex of the parabola then, $A = B = 0$

$$F = -i\tfrac{1}{2}g\alpha^2 \qquad \text{---(III)}$$

also $$\bar{F} = i\tfrac{1}{2}g\alpha^2$$

To find the complex potential for this flow substitute in equation II thus,

$$\frac{dw}{d\alpha} = (g\alpha)^2$$

$$w = \tfrac{1}{3}g^2\alpha^3 + D$$

Let α take complex values $\alpha = a + ib$ and if $w = 0$ at the apex of the parabola $D = 0$ and

$$w = \Phi + i\psi = \tfrac{1}{3}g^2(a + ib)^3$$

$$\Phi = \tfrac{1}{3}g^2(a^3 - 3ab^2)$$

$$\psi = \tfrac{1}{3}g^2(3a^2b - b^3) \qquad \text{---(IV)}$$

Equation III is now used to obtain the general $z - \alpha$ relationship for complex values of α

$$z = x + iy = -i\tfrac{1}{2}g(a + ib)^2$$

$$x = gab$$

$$y = -\tfrac{1}{2}g(a^2 - b^2) \qquad \text{---(V)}$$

To plot stream lines (or equipotentials) equations IV give the relationship between a and b for constant values of ψ (or Φ). Values of a and b thus obtained are substituted in equations V to give points (x,y) on the stream line (equipotential line) in the physical z-plane. Figure 6 shows the flow pattern thus obtained. The flow is divided into four distinct regions as indicated by the arrows showing the direction of flow in each region. A practical application for such a flow is difficult to imagine.

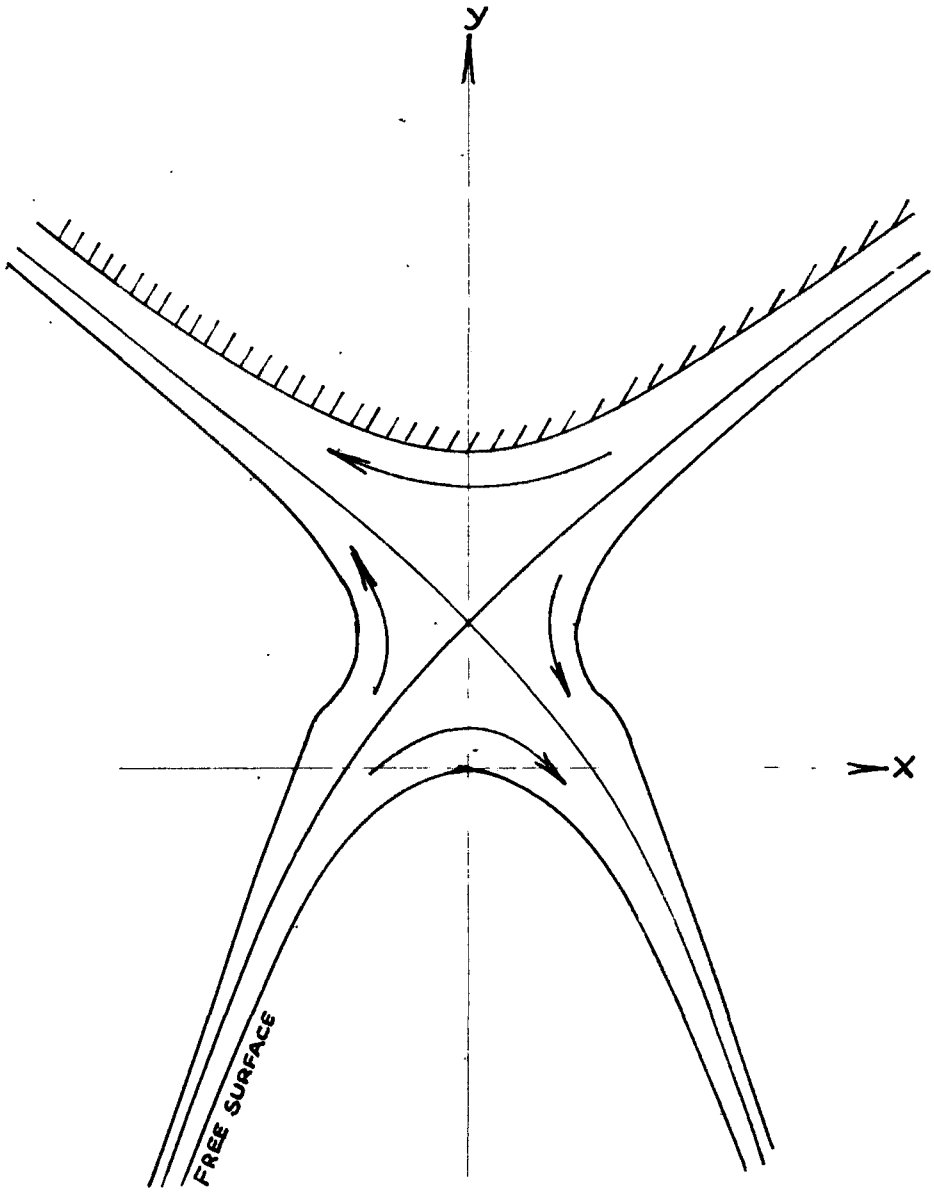

FIGURE 6

FLOW WITH A

PARABOLIC FREE SURFACE

APPENDIX B

CALCULATION OF A_{jk} WHEN $j = k$

When $j = k$ the integrand is infinite, but the contribution to the summation of the increment $(\Delta r)_k$ containing this point is finite. An average value of the integrand based on pure integration must, therefore, be inserted into the integrand matrix when $j = k$. The assumption is made that over this increment the relationship between r and $\frac{\beta_k}{\beta_j}$ is linear, and the integration is carried out between limits γ_1 and γ_2 where $\frac{\beta_k}{\beta_j} = \gamma$.

Note that when $\gamma > 1$

$$\tanh^{-1}\gamma = \tanh^{-1}\frac{1}{\gamma} + i\frac{\pi}{2}$$

In the integration the real part of the integrand only is dealt with, and the integration must in fact be evaluated in two stages between the limits γ_1 to 1, and $\frac{1}{\gamma_2}$ to 1 (Figure 7).

$$\int_{\gamma_1}^{1} \tanh^{-1}\gamma \, d\gamma = \left| \gamma \tanh^{-1}\gamma + \tfrac{1}{2}\log(1 - \gamma^2) \right|_{\gamma_1}^{1}$$

To evaluate the upper limit substitute $1 - \varepsilon$ for 1 and let $\varepsilon \to 0$

$$\lim_{\varepsilon \to 0} \left\{ (1 - \varepsilon)\tanh^{-1}(1 - \varepsilon) + \tfrac{1}{2}\log\left[1 - (1 - \varepsilon)^2\right] \right\}$$

$$= \lim_{\varepsilon \to 0} \left\{ (1 - \varepsilon)\tfrac{1}{2}\log\frac{1 + (1 - \varepsilon)}{1 - (1 - \varepsilon)} + \tfrac{1}{2}\log\left[1 - (1 - \varepsilon)^2\right] \right\}$$

$$= \underset{\varepsilon \to 0}{\text{Limit}} \left\{ (1 - \varepsilon) \tfrac{1}{2} \log \frac{2 - \varepsilon}{\varepsilon} + \tfrac{1}{2} \log (2\varepsilon - \varepsilon^2) \right\}$$

$$= \tfrac{1}{2} \log \left(\frac{2}{\varepsilon} \cdot 2\varepsilon \right)$$

$$= \log 2$$

Therefore

$$\int_{\gamma_1}^{1} \tanh^{-1} \gamma \, d\gamma = \log 2 - \{ \gamma_1 \tanh^{-1} \gamma_1 + \tfrac{1}{2} \log (1 - \gamma_1^2) \}$$

Similarly

$$\int_{\frac{1}{\gamma_2}}^{1} \tanh^{-1} \gamma \, d\gamma = \log 2 - \left\{ \frac{1}{\gamma_2} \tanh^{-1} \frac{1}{\gamma_2} + \tfrac{1}{2} \log \left[1 - \left(\frac{1}{\gamma_2} \right)^2 \right] \right\}$$

The total contribution to the summation at $j = k$ is the sum of these two expressions and the increment is $(1 - \gamma_1) + (1 - \frac{1}{\gamma_2})$. Hence the "average ordinate" value to be placed in the integrand matrix is,

$$A_{kk} = \frac{2 \log 2 - \left\{ \gamma_1 \tanh^{-1} \gamma_1 + \tfrac{1}{2} \log (1 - \gamma_1^2) + \frac{1}{\gamma_2} \tanh^{-1} \frac{1}{\gamma_2} + \tfrac{1}{2} \log \left[1 - \left(\frac{1}{\gamma_2} \right)^2 \right] \right\}}{(1 - \gamma_1) + (1 - \frac{1}{\gamma_2})}$$

The values of γ_1, γ_2 in a particular instance can be obtained with sufficient accuracy by interpolating between 1 and the neighbouring values of γ corresponding to the ends of the potential interval.

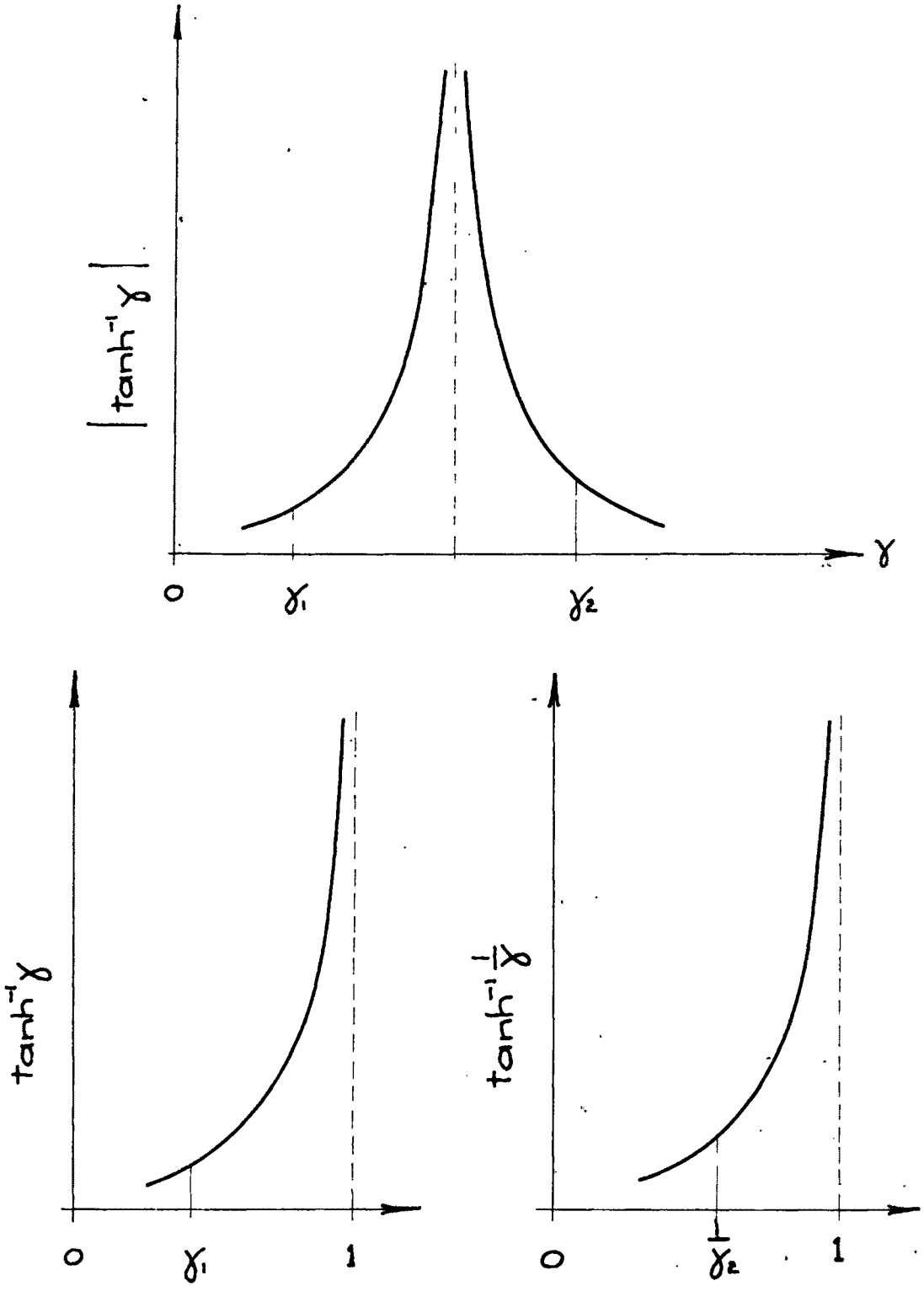

FIGURE 7

BEHAVIOUR OF A_{jk} NEAR $j = k$

APPENDIX C

DERIVATION OF THE JET THICKNESS EQUATION

Consider the free body of liquid isolated by sections AA and BB far upstream and far downstream respectively (Figure 8). AA is far enough upstream so that the flow there may be considered uniform at critical depth. The pressure distribution across AA can then be assumed hydrostatic. BB is a right section of the jet far enough downstream for the pressure across BB to be considered constant and equal to the external pressure on the free boundaries. h is the average depth of this section below the "total energy line" and the section makes angle $\bar{\theta}$ with the vertical. The average velocity across this section can then be written as

$$q = \sqrt{2gh}$$

Flow across AA = Flow across BB

$$y_o q_o = \frac{\Delta h}{\cos \bar{\theta}} \sqrt{2gh}$$

The flow across AA is critical, therefore,

$$q_o = \sqrt{g y_o}$$

Hence

$$h = \frac{\cos^2 \bar{\theta}}{2(\Delta H)^2} y_o^3 \qquad \text{---(I)}$$

Rate of change of horizontal momentum between AA and BB

= force on AA (the channel bed is considered smooth)

$$2 g \rho h . \Delta h - g \rho y_o^2 = \tfrac{1}{2} \gamma y_o^2$$

$$h = \frac{3}{4} \frac{y_o^2}{\Delta h} \qquad \text{---(II)}$$

Equating (I) and (II) obtain

$$\Delta h = \frac{2}{3} y_o \cos^2 \bar{\theta}$$

or in the unit model this is

$$\Delta h = \frac{2}{3} \cos^2 \bar{\theta}$$

$$\text{jet thickness} = \frac{\Delta h}{\cos \bar{\theta}} = \frac{2}{3} \cos \bar{\theta}$$

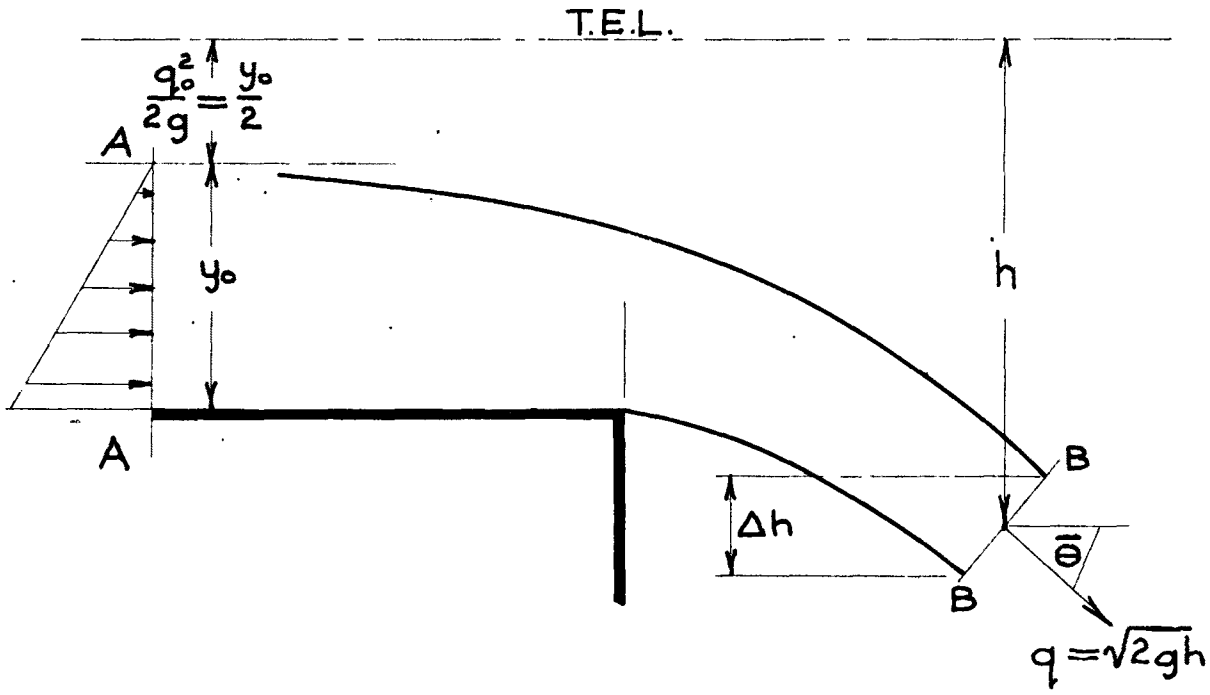

FIGURE 8

JET THICKNESS OF

THE FREE OVERFALL

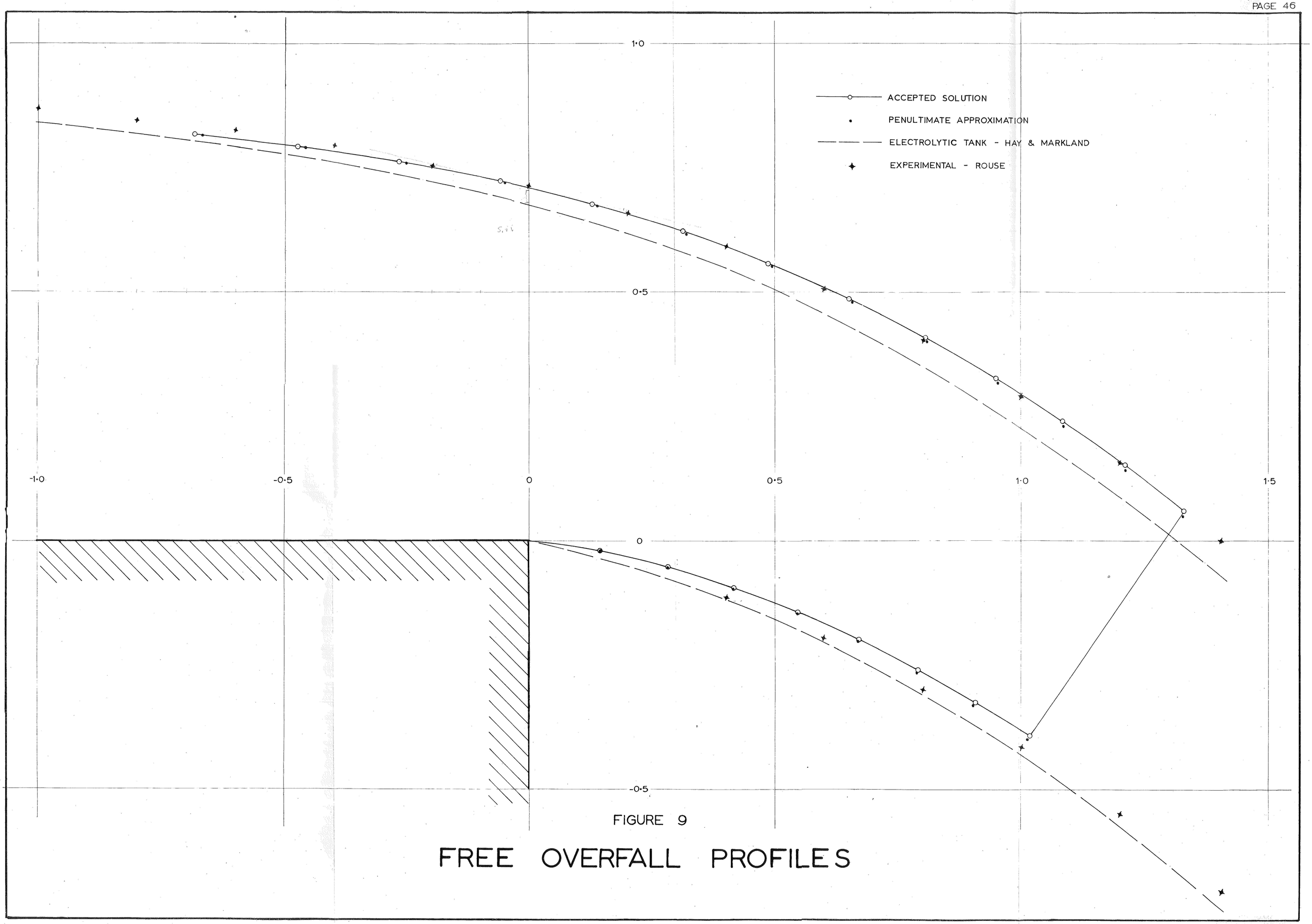

FIGURE 9

FREE OVERFALL PROFILES